Research Article | Vol. 30, No. 11 / 23 May 2022 / Optics Express 19005
Optics EXPRESS

Terahertz continuous wave spectroscopy: a portable advanced method for atmospheric gas sensing

ANNALISA D'ARCO,[1,2,3] DANIELE ROCCO,[1] FERNANDO PIAMONTE MAGBOO JR.,[1] CANDIDA MOFFA,[4] GIANCARLO DELLA VENTURA,[3,5,6] AUGUSTO MARCELLI,[3,7] LUIGI PALUMBO,[1,8] LEONARDO MATTIELLO,[1] STEFANO LUPI,[2,3] AND MASSIMO PETRARCA[1,8,*]

[1]*SBAI, Department of Basic and Applied Sciences for Engineering, University of Rome 'Sapienza', Via Scarpa 16, 00161 Rome, Italy*
[2]*Physics Department, University of Rome 'Sapienza', P.le Aldo Moro 5, 00185 Rome, Italy*
[3]*INFN-LNF Laboratori Nazionali Frascati, Via E. Fermi 54, 00044 Frascati, Italy*
[4]*Department of Environmental Biology, University of Rome 'Sapienza', P.le Aldo Moro 5, 00185 Rome, Italy*
[5]*Department of Science, University Rome Tre, V.le G. Marconi 446, 00146, Rome, Italy*
[6]*INGV, Via di Vigna Murata 605,00143, Rome, Italy*
[7]*Rome International Centre for Materials Science Superstipes, Via dei Sabelli 119A, 00185, Rome, Italy*
[8]*INFN – Section of Rome 'Sapienza', P.le Aldo Moro 2, 00185 Rome, Italy*
[*]*massimo.petrarca@uniroma.it*

Abstract: Motivated by the increasing demand to monitor the air-quality, our study proved the feasibility of a new compact and portable experimental approach based on Terahertz (THz) continuous wave high resolution spectroscopy, to detect the presence of the air's contaminants as greenhouse gases (GHG) and volatile organic compounds (VOCs). In this specific work, we first characterized, determining their molar absorption coefficient in the spectral region (0.06-1.2) THz, the pure optical response of the vapor of five VOCs: methanol, ethanol, isopropanol, 1-butanol and 2-butanol. In particular, 1-butanol and 2-butanol are characterized for the first time in literature at THz frequencies. Then we studied the optical response of their mixtures achieved with ambient air and ethanol. The results show that it is possible for a differentiation of single components by describing their spectral absorption in terms of the linear combination of pure compounds absorption. This proof of concept for this apparatus study and set-up paves the way to the use of THz Continuous wave high resolution spectroscopy for the environmental tracking of air pollutants.

1. Introduction

Volatile organic compounds (VOCs) belong to the family of toxic chemicals, such as hydrocarbons, alcohols, nitrogen-based compounds produced by natural and/or anthropogenic sources [1–3]. They are considered to be within the main indoor and outdoor air chemical contaminants [4–7] because, due to their low boiling points, they evaporate even at room temperature rapidly diffusing in the environment [5]. For this reason, they are now considered as an important risk factor for health and safety [6–9]. Therefore, the detection of VOCs for monitoring the indoor and outdoor air-quality is a topical issue. In these last years, the increasing demand for gas sensing systems and devices triggered the technological advances [10–13]. There are various conventional and innovative analytical methods for VOCs detection, based on chemical and physical principles, i.e. gas chromatography, mass spectroscopy [14–16], optical, electrochemical piezoelectric and

#456022 https://doi.org/10.1364/OE.456022
Journal © 2022 Received 11 Feb 2022; revised 22 Mar 2022; accepted 5 Apr 2022; published 16 May 2022

Optics EXPRESS

chemo-sensors [11,17–21]. Many of the above-mentioned methods measure the exposure to chemical agents using static samplers and/or analytical techniques that require complex off-line procedures, time-averaged response with reduced sensitivity. The electrochemical piezoelectric and chemo-sensors have gained popularity thanks to their operational simplicity, suitability for point-of-care, their small size and high sensitivity. Nevertheless, high sensitivity is achieved for high operation temperature, see for example the electrochemical sensors [22,23], and this represents a risky condition for the detection of inflammable gases. VOCs' complementary detection methods are based on vibrational spectroscopy. The optical gas sensing systems based on vibrational spectroscopy guarantee detection limits comparable with gas chromatography and can overcome the issues related to chemo-resistive gas sensors [10,24]. Very recently, Terahertz spectroscopy (0.1-10 THz) attracted increasing interest, strongly encouraged by the rapid technological developments [25–28]. This spectroscopy, in fact, has been successfully applied in various technological and scientific fields e.g. biomedicine, condensed matter [29], analytical chemistry [30–34], including the gas sensing [10,35]. Compared to conventional infrared techniques used for gas sensing, THz spectroscopy shows many advantages: unique properties of high penetration in dielectric material, low aerosol scattering losses [36] and low photon energy (i.e. 4 meV @ 1 THz) which assures no molecules ionization and no combustion of inflammable materials. Moreover, THz spectroscopy is insensitive to the thermal background, showing a high Signal-to-Noise Ratio (SNR) and it does not require cooled detectors. Thanks to all these advantages THz spectroscopy may provide selective non-intrusive identification of gas molecules, through their molecular roto-vibrational modes, ensuring a high chemical selectivity and sensitivity and therefore it can represent a novel tool to probe the presence of VOCs in their gas-phase. The first experimental evidence to this issue was provided by a study on acetonitrile (CH_3CN) gas in the presence of smoke at atmospheric pressure. Many rotational transitions were resolved in the spectral range between (0.1-1) THz, without the influence of scattering and/or absorption by the smoke [37]. In addition, the detection of hazardous gases generated by the combustion process, such as hydrogen cyanide (HCN) and H_2O molecules due to a urethane foam block [38], suggested possible applications in remote locations. Choi et al. [39] detected the presence of low concentrations of di-nitrogen monoxide (N_2O, 25% in air) with a 1-m-long gas cell, while monitoring via remote detection, nitrogenous compounds (N_xO_y). The results opened the possibility of applying THz spectroscopy for the identification [39]. THz time-domain spectroscopy (THz-TDS) has been first applied in gas sensing, demonstrating a higher selectivity compared to infrared spectroscopy in the examination of various gases, such as acetaldehyde (C_2H_4O), acetonitrile (C_2H_3N), NH_3, propionaldehyde, propionitrile (C_3H_5N), and H_2O vapor in the range between (0.03–3.9) THz [40]. Although nowadays, THz-TDS has become the common tool for the material analysis, the achievable spectral resolution represents a limitation for some specific applications like gas-phase sensing in environment monitoring [10], human breath [41–43] and drugs and explosives detection [39,44], where high resolution THz continuous wave frequency-domain spectroscopy (THz-FDS) is highly demanded. THz-FDS is closely related to TDS in physical processes, measurement and detection schemes [45,46]. In comparison to the TDS, the main advantages of FDS are the high frequency resolution (~ MHz), the possibility to work at a fixed frequency or in a tunable frequency range and the relatively low cost. Moreover, THz-FDS systems do not require mechanical movements and therefore are more stable, compact and portable, thus suitable for real-time *in situ* measurements [47,48]. In this work, we experimentally investigated the optical response of a set of alcohols, belonging to the VOCs' family and of interest as toxic contaminants posing a risk to the human health, in gas-phase. We applied THz-FDS spectroscopy with a broad bandwidth (60-1200) GHz and high resolution of 0.1 GHz. Despite the great interest shown in THz gas-sensing, many gas-phase VOCs have never been spectrally characterized with high resolution in the THz frequency range (60-1200) GHz, and few research activities were focused on the detection in

Optics EXPRESS

ambient air [31,42,49–51]. Thus, we first studied the optical response of these pure compounds in gas-phase: methanol, ethanol, isopropanol, 1-butanol and 2-butanol, indicated in the following text and figures, respectively, as MeOH, EtOH, IsoOH, BuOH-1 and BuOH-2. Then we studied the optical behavior of BuOH-2/air mixtures by increasing progressively the air content and BuOH-1/EtOH mixture. To our knowledge, this is the first high resolution characterization for BuOH-1, BuOH-2 and the mentioned mixtures in this THz spectral region. The results of this study prove that this methodology can be capable of gas sensing in a fashionable and compact set-up which can be carried on for *in situ* atmospheric measurements.

2. Materials and methods

2.1. Materials

The following liquid VOC samples were used: methanol (CH_3OH - Sigma Aldrich - Purity ≥99.8%), ethanol (C_2H_6O - Sigma Aldrich - Purity ≥99.8%), isopropanol ($CH_3CH(OH)CH_3$ - Sigma Aldrich - Purity ≥99.9%, 1-butanol ($CH_3(CH_2)_3OH$ - Sigma Aldrich - Purity ≥99.5%) and 2-butanol ($CH_3CH(OH)CH_2CH_3$ - Sigma Aldrich - Purity ≥99.5%). The binary mixture of BuOH-1 and EtOH was prepared blending 50% in volume of both alcohols. The mixture of BuOH-1/EtOH was injected into the absorption gas cell, waiting for the equilibrium liquid-gas condition to be reached. The total pressure of 15 mbar was measured. Concerning the BuOH-2/air mixtures, we injected the liquid VOCs into the absorption gas cell, waiting for the equilibrium condition (liquid-vapor) to be reached. This condition was monitored by the Alcatel Pirani CA 111 gauge. Subsequently, different volumes of ambient air (relative humidity RH=40%) were added to the gas cell.

2.2. Methods

In order to investigate the spectral features of gaseous samples in the frequency range (60-1200) GHz, we used a commercial THz-FDS (TeraScan 1550, TOPTICA Photonics AG, Germany) system, as shown in Fig. 1. The system includes two distributed feedback (DFB) lasers (#LD-1550-0040-DFB at 1533 and at 1538 nm), one THz transmitter (TX) and THz receiver (RX), four off-axis parabolic mirrors (PMs) and a signal processing unit. The lasers are coupled by optical fibers into a laser combiner (Fib-MIX) to generate a beat signal which is divided into two beams with the same average power approximately of 35 mW. One of the two beat signals pumps the TX, a low-temperature grown InGaAs photoconductive antenna (PCA), generating THz radiation though photomixing technique [35,52]. The generated THz beam signal is collimated by a PM and then recollected and focused on the RX which is also coupled by a silicon super hemisphere lens. The detected THz signal drives the photo-carriers pumped by the other laser beat to form a photocurrent amplified by a lock-in amplifier (LIA). The TX is biased by an AC modulation frequency of ∼ 39.67 kHz and voltage 0.9 V. The detected continuous wave (CW) THz spectrum covers the range (60-1220) GHz with an intensity I(ν) decreasing with increasing frequency as shown in Fig. 1(c) blue curve (bands for the blue curve are related to water vapor absorption). This decreasing behavior is an intrinsic characteristic of the TX/RX emitter/detector response [35]. The homemade gas cell was designed and realized in order to meet the requirements of the system. It is equipped with 2 mm thick Teflon windows, which were located perpendicular to the collimated radiation transmission direction, and with a Pirani sensor as vacuum gauge. The gas cell is 50 mm long and has an inner diameter of 30 mm, enabling the collimated THz beam to completely pass through the cell without clipping losses.

We performed the measurements at room temperature (measured 20 °C). To minimize the water vapor absorption due to the THz beam path outside the gas cell, we closed the optical set-up in an acrylic box, containing a drying air system that maintained the humidity at 20%. Background collections (I_{cell}: empty gas cell) were performed immediately prior of each sample.

Optics EXPRESS

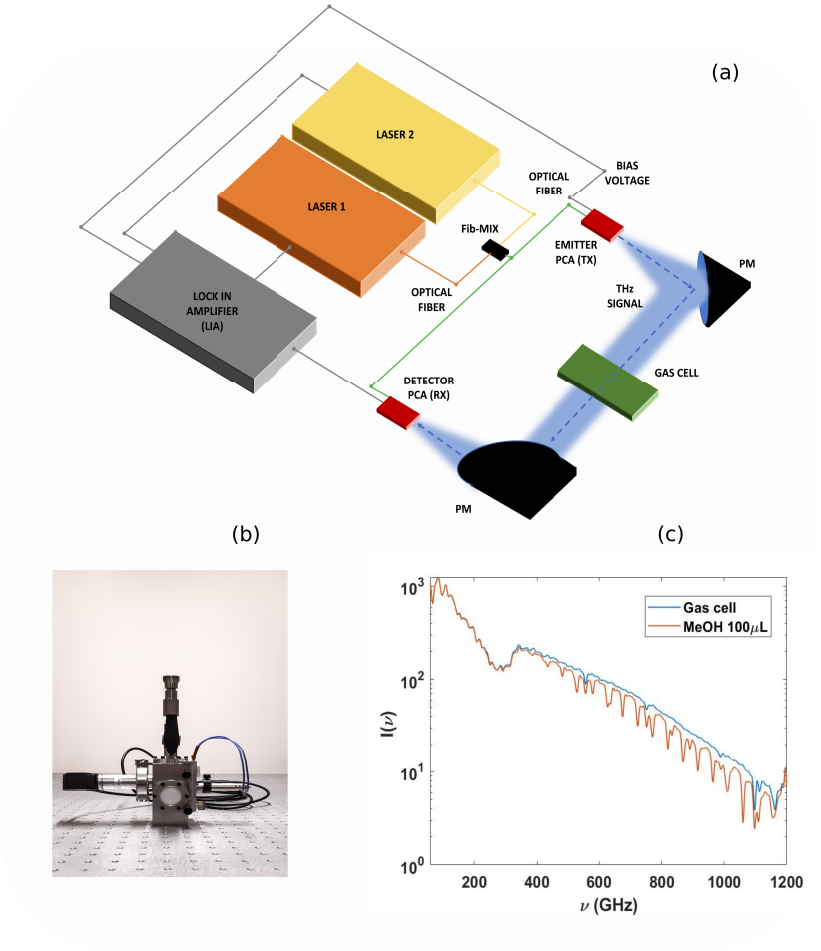

Fig. 1. (a) Schematic layout of THz-FDS system for gas detection. (b) Home-made gas absorption cell. (c) THz intensities as a function of frequency of empty (blue) and filled gas cell with MeOH (red), respectively. The minima appearing in the blue curve are related to water vapor absorption, for the red line to the MeOH absorption.

Optics EXPRESS

The compound to be analyzed was injected into the bottom of the gas cell in its liquid state (natural state at room temperature and ambient pressure). Then, we monitored the vapor pressure by the Pirani gauge. Once the equilibrium (liquid-vapor) is reached, we collect the data (I_{sample}) for the sample. Each spectrum was acquired between 60 to 1200 GHz with a frequency resolution of 0.1 GHz and integration time of 30 ms. Raw data were processed and analyzed using algorithms written by the authors in MATLAB (ver. 2019a, MathWorks Inc., USA) as interpreter. The Beer–Lambert law is used to relate the amount of THz radiation transmitted through the gas cell. The experimental absorbance is calculated by

$$Absorbance = -log(I_{sample}/I_{cell}) \tag{1}$$

the absorbance is also directly proportional to the optical path d of the gas cell and the concentration of the sample, as follows

$$Absorbance = \alpha_M Cd \tag{2}$$

the inverse formula combined with the perfect gas law gives

$$\alpha_M = Absorbance/Cd = AbsorbanceRT/Pd \tag{3}$$

where α_M [cm^{-1}] is the molar absorption coefficient dependent on pressure and temperature, C is a molar concentration [M], d [cm] is the optical path of the gas cell, R the gas constant, T [K] the temperature and P [mbar] the pressure.

3. Results and discussions

3.1. Absorption of pure alcohols

The measured molar absorption coefficient α_M of the vapor of the pure MeOH, EtOH, IsoOH, BuOH-1 and BuOH-2 are displayed in Fig. 2(a and b). The absorption spectra are referred to the vapor concentration at equilibrium of 100 μl of the compound in its liquid state, injected inside the gas cell at the temperature of 20 °C. We monitored the equilibrium state by measuring the pressure.

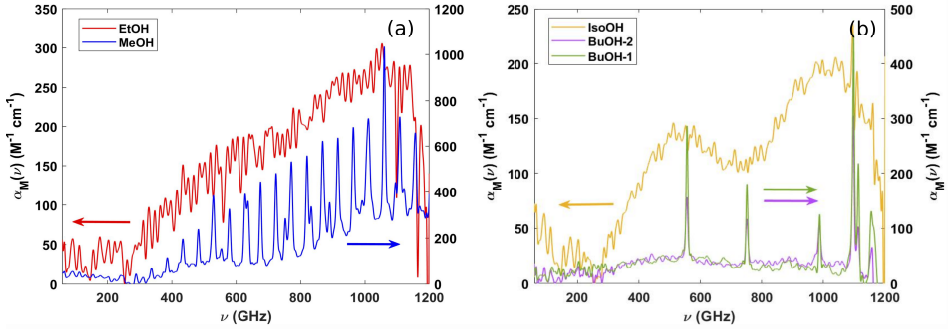

Fig. 2. Measured molar absorption coefficients of pure alcohols as a function of frequency: (a) MeOH and EtOH, (b) IsoOH, BuOH-1 and BuOH-2 in the spectral range (60-1200) GHz.

Inspection of Fig. 2 reveals grouping of the gas-phase components with strong rotational absorption features, such as MeOH and EtOH (Fig. 2(a)) that dominate the spectra compared to BuOH-1 and BuOH-2 (Fig. 2(b)). MeOH is one of the most abundant oxygenated VOCs present in the atmosphere [53]. We selected methanol as the gas sample to demonstrate the capability of the THz-FDS system to simultaneously probe multiple absorption lines, as made in other works [37,40,42]. The rotational spectral shape is evident and the lines corresponding to rotational

Optics EXPRESS

transitions are spaced approximately every 50 GHz. MeOH is a prolate symmetric top molecule and the frequency spacing approaches 2B=49.38 GHz [54]. EtOH has a lower α_M than MeOH and shows periodic features distributed at approximately equal distance, see Fig. 2(a). As well as for MeOH, EtOH is a prolate asymmetric top molecule with rotational constants A=34.02 GHz, B=9.19 GHz and C=8.10 GHz [55]. As the difference 2B-2C ~ 1.09 GHz (degeneracy) is lower than the Full Width at Half Maximum FWHM ~ 9 GHz of the rotational transitions, in Fig. 2 the spectra do not allow discriminating between the two features. Due to the same degeneracy effect the rotational pattern connected to the A rotational constant is likely to be superimposed to the other two (B,C). In Fig. 2(b), we show α_M for alcohols with a long carbon chain (≥3), including IsoOH, BuOH-1 and BuOH-2. All of them exhibit a low α_M compared to MeOH. The rotational constants for the IsoOH, A=8.49 GHz, B=8.04 GHz and C=4.77 GHz, suggest that the molecule can be considered as an oblate asymmetric top [56]. The experimental frequency spacing of the spectral lines is ~ 16 GHz. As before, the difference 2A-2B ~ 0.45 GHz (degeneracy) is lower than the FWHM ~ 5 GHz of the rotational transitions and again in Fig. 2(b), thus we cannot discriminate the two. Due to the same degeneracy effect the rotational pattern connected to the C rotational constant is again superimposed to the other two (A,B). BuOH-1 and BuOH-2 show a lower absorption with respect to the other three examined alcohols. Despite the butanol isomers share the same chemical formula (C_4H_9OH), their physical properties such as melting point and molar volume are different from those of the other isomers. The butanol isomers have different chemical configurations due to the arrangement of the methyl groups with respect to the carbon attached to the hydroxyl group. The chemical structure results in different spectral shapes, as demonstrated in the IR spectral region [57]. Here, for the first time, we observed different absorption characteristics between BuOH-1 (green line) and BuOH-2 (purple line), (Fig. 2(b)) by THz-FDS. We evaluated their main THz frequency positions using the second-derivative analysis [58,59], that shows a negative peak for each band and a shoulder in the absorption spectrum. Very strong bands appear at 556.9, 751.9 and 988 GHz for BuOH-1. For BuOH-2, these peaks are shifted at 556.5, 751.4 and 987.4 GHz, as evident in the limited frequency interval of Fig. 3(a). These bands can be associated to hydroxyl groups rotational modes. The relative shifts of the main peaks of BuOH-1 and BuOH-2 are even more evident if we refer to their second-derivatives for the three sub-band frequencies, as reported in Fig. 3(c)-e. For each single compound, the second-derivatives are given, and the negative peaks identify the main absorption bands for BuOH-1 and BuOH-2, respectively. A significant shift of 500 MHz is observed in BuOH-2, attributable to the different isomeric molecular structure of BuOH-1 compared to BuOH-2. In addition, as the background line for the BuOH-1 and BuOH-2 is comparable, we can give a quantitative estimation of the absorption values: α_M at 557 and 752 GHz for BuOH-1 is 2-fold greater than for BuOH-2, instead for the absorption at 988 GHz they are at 132 $M^{-1}cm^{-1}$ and 102 $M^{-1}cm^{-1}$ for BuOH-1 and BuOH-2, respectively.

3.2. Absorption of binary mixture of BuOH-2 and air

To further investigate the applicability of the THz-FDS system as a valid alternative tool for gas sensing in a system approaching those found in ambient air, we performed the absorption measurements for the BuOH-2/air mixtures. We fixed the concentrations of BuOH-2 gas into the gas cell and varied progressively the air content, injecting fixed volumes (3 ml and 6 ml) at 40% RH and 20°C room temperature. In Fig. 4(a), we report the experimental absorbances for the mixtures of BuOH-2/air. Increasing the air content, it is possible to observe different absorption behaviours.

At low frequencies, between 100-350 GHz, the absorbance tends to increase compared to the pure compound. This may be due to strongest water vapor rotational lines and pressure broadening effects [51]. Moreover the 10 GHz periodicity, which is characteristic of the pure BuOH-2 compound, tends to disappear and a new frequency modulation approximately at 20

Optics EXPRESS

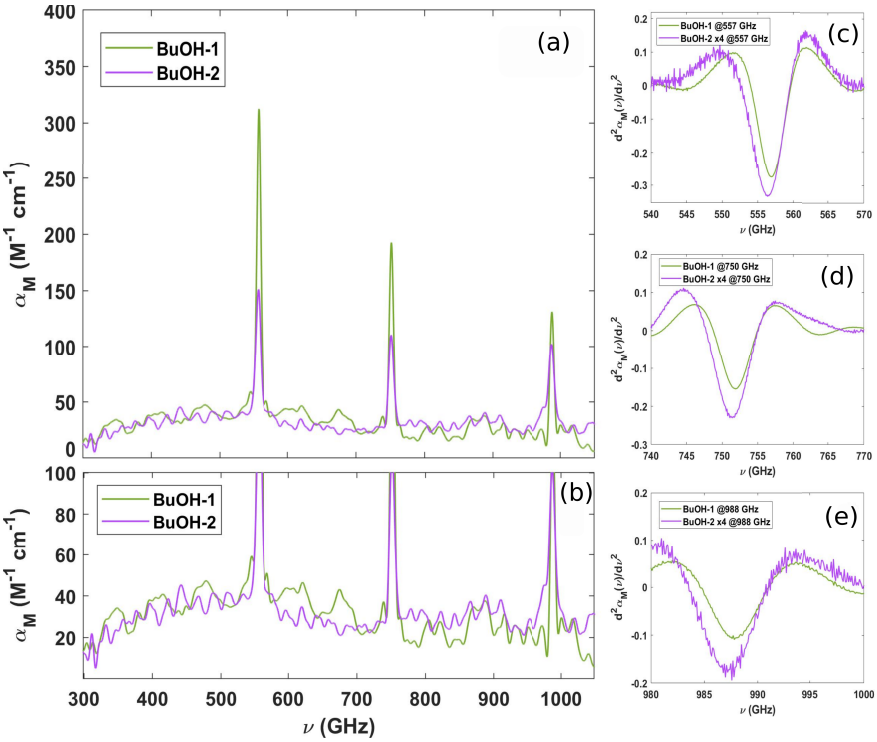

Fig. 3. (a) The frequency sub-bands of α_M for BuOH-1 (green line) and BuOH-2 (purple line) between (300-1000) GHz. (b) Enlargement of the lower intense spectral components in this spectral region. (c) (d) and (e) Second-derivatives of the absorption spectra of BuOH-1 and BuOH-2 in the frequency positions close to 557 GHz, 752 GHz and 988 GHz, respectively.

GHz appears. Concerning the most intense absorption lines, located around 556.5, 751.4 and 987.4 GHz, we do not observe appreciable shifts, but only a change in their intensity. For the sub-bands at 556.4 and 751.4 GHz we note a progressive increase in intensity as a function of the increase in the air content in the mixture, evident in Fig. 4(b) and 4(c), where the integrated areas of the main peaks (after subtraction of the background) are reported. The subtraction has been performed with a spline curve [59]. A different behaviour is observed for the absorption band located at 987.4 GHz (Fig. 4(d)). In fact, this band tends to be split into three sub-bands at around 973.7, 986.9 and 997 GHz when the air content increases up to about 6 ml.

3.3. Absorption of binary mixture of BuOH-1 and EtOH alcohols

We have prepared 200 μl of solution mixing equal volumes of components, but with molar fractions, 0.6129 ± 0.0001 and 0.3907 ± 0.0001 of EtOH and BuOH-1, respectively. The experimental net absorbance of the gaseous mixture is the sum of the contribution of the linear absorbance of each component, when the interaction among components can be considered negligible; this is known as the multiple absorbers approach [51]. The experimental absorbance for non-interacting compounds can be written as

$$A_{mix}^{exp} = \sum A_i \tag{4}$$

where A_{mix}^{exp} is the experimental mixture absorbance and A_i is the estimated pure absorbance due to each species i, at the same pressure and temperature conditions. The measured net absorbance

Optics EXPRESS

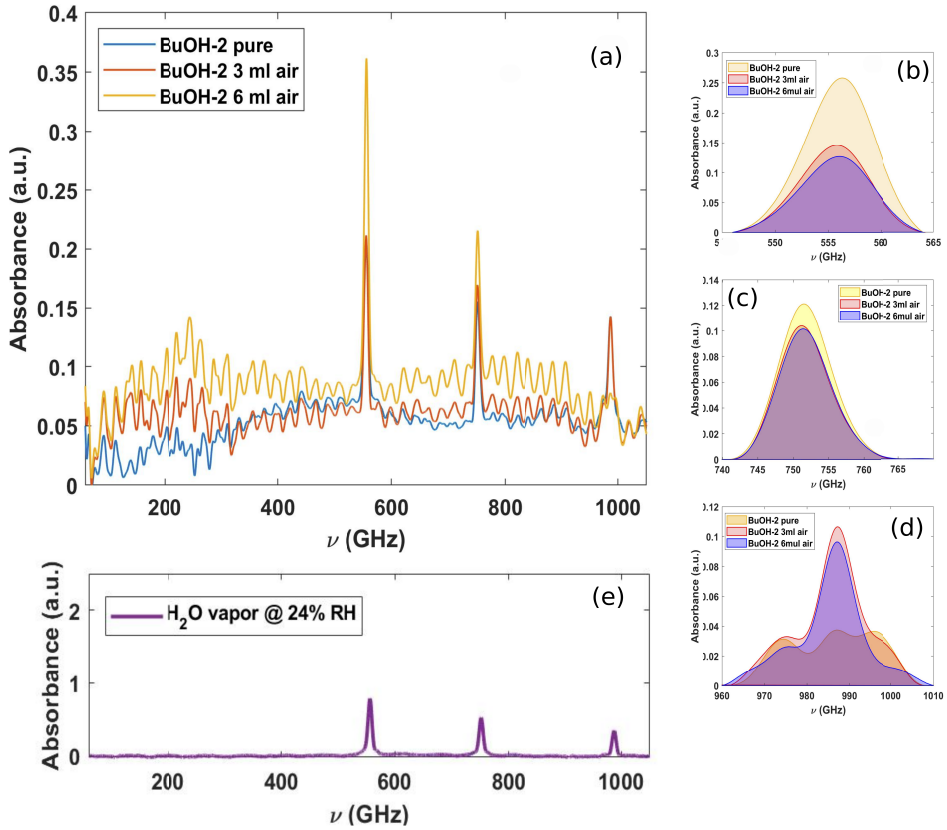

Fig. 4. (a) Experimental absorbances of pure BuOH-2 and BuOH-2/air mixtures. (b), (c) and (d) the integral areas of specific sub-band frequencies at 557 GHz, 751 GHz and 988 GHz, respectively. For the first sub-band frequencies at 557 and 751 GHz a reduction of integrated areas is visible. Observing the sub-band frequency at 988 GHz as the air content grows, a strong spectral modification appears, with the formation of new frequency peaks at around 973.7, 986.9 and 997 GHz. (e) Experimental absorbance of air at 24% RH.

A_{mix}^{exp} is given by

$$A_{mix}^{exp} = A_{BuOH}x_1 + A_{EtOH}x_2 + x_3 \tag{5}$$

where x_1, x_2 are the weights considering the species concentrations in the gas mixture and x_3 a parameter required considering the background, due to any systematic errors associated to the loading gas cells procedures, noise, etalon effect, etc.. Figure 5 illustrates the comparison between the measured absorbance of the binary mixture (blue line) and the absorbance obtained as a weighted linear combination of the measured spectra (dotted red line) for the pure components in the spectral range (60-1000) GHz.

The residual difference reported in Fig. 5(b), shows a good agreement between the experimental mixture absorbance and the weighted linear combination of the pure compounds therefore confirming the validity of the data.

Optics EXPRESS

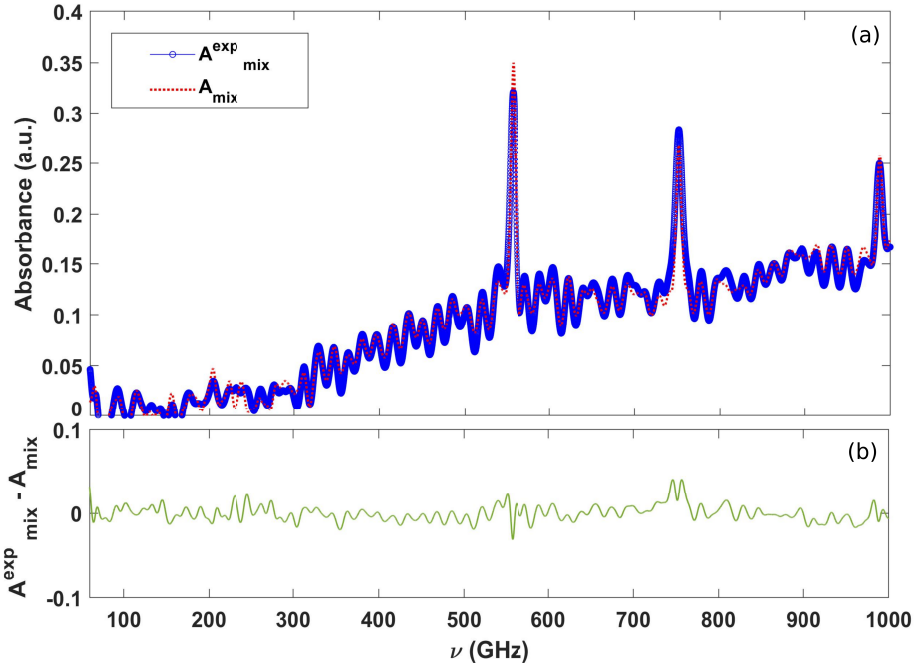

Fig. 5. (a) Comparison of the experimental absorbance of BuOH-1/EtOH mixture at 15 mbar total pressure with the weighted sum of measured absorbances for pure BuOH-1 and EtOH at the same pressure and temperature. (b) residual difference between the experimental absorbance vs. the calculated one. The root-mean-square (RMS) deviation is 0.007.

4. Conclusions

In this work, we experimentally explored the spectral characteristics of five alcohols in the frequency range (60-1200) GHz by using high-resolution THz-FDS spectroscopy. The spectral characterization of these selected VOCs, under controlled conditions of pressure, temperature and RH, allowed the quantitative evaluation of their molar absorption coefficients and the recognition of specific spectral features for each compound. Our attention has been particularly focused on the two isomeric forms of butanol, BuOH-1 and BuOH-2, which to our knowledge, have never been characterized in the THz spectrum in the gaseous phase. For them, we were also able to identify spectral differences for the intense main peak at 0.5 GHz between BuOH-1 and BuOH-2, attributable to the arrangement of the methyl groups with respect to the carbon attached to the hydroxyl group. Moreover, we studied the spectral absorption measurements for the mixtures alcohol/air and alcohol/alcohol. In particular, the BuOH-2/air mixture absorbances, compared to the pure BuOH-2 one, increase in all the spectral region as the air content grows. At lower frequencies, we noticed a modification of the spectral pattern. Finally, we studied the optical response in the THz regime for the alcohol-mixture (BuOH-1/EtOH). The spectral absorption measurement for the BuOH-1/EtOH mixture was compared with the weighted linear combination of independently acquired pure compound spectra, achieving a good agreement.

Our results prove that THz-FDS is a reliable methodological high-resolution approach in the gas sensing, for applications in human breath analysis and environmental/occupational monitoring [60] and corroborate the great potentiality of THz-FDS for the quantitative evaluation of VOCs contents in the multiple-component mixtures. In addition, the assembled measurement unit adopted for this work is compact, light and does not require high power consumption. For these reasons it can be easily adopted for *in situ* measurements and implementable for remote-distance

Optics EXPRESS

monitoring. In order to increase the selectivity and sensitivity of the THz-FDS sensing system, it is possible to implement a platform to collect and accumulate large amounts of chemicals that are diluted in the air [10,11,61–63]. Furthermore, the data analysis of this spectroscopic methodology can be equipped with advanced computational analyses: network analysis, machine learning, and principal components analysis algorithms [64] allowing for a back-door robust post-processing for the spectral interpretation and pattern recognition necessary for fast detection of gaseous chemicals [60].

Acknowledgments. This research was supported by the Ph. D. funding in the framework of "Programma Operativo Nazionale (PON) - Ricerca e Innovazione 2014-2020 - Azione IV.5 - Dottorati su tematiche green – FSE REACT-EU and by "Sapienza" University of Rome grant. This research was carried out also in the framework of the BRIC-INAIL project ID12. This work was also supported by the NATO Science for Peace and Security Programme under grant No. G5889 – "SARS-CoV-2 Multi-Messenger Monitoring for Occupational Health & Safety-SARS 3M" and by LazioInnova "Gruppi di Ricerca 2020" of the POR FESR 2014/2020 - A0375-2020-36651 project titled "DEUPAS - DEterminazione Ultrasensibile di agenti PAtogeni mediante Spettroscopia".

Disclosures. "The authors declare no conflicts of interest."

Data availability. Data underlying the results presented in this paper are not publicly available at this time but may be obtained from the authors upon reasonable request.

References

1. F. Khan and A. Ghoshal, "Removal of volatile organic compounds from polluted air," J. Loss Prev. Process Ind. **13**(6), 527–545 (2000).
2. H. Zhang, Y. Shen, W. Liu, Z. He, J. Fu, Z. Cai, and G. Jiang, "A review of sources, environmental occurrences and human exposure risks of hexachlorobutadiene and its association with some other chlorinated organics," Environ. Pollut. **253**, 831–840 (2019).
3. V. Longo, A. Forleo, A. Ferramosca, T. Notari, S. Pappalardo, P. Siciliano, S. Capone, and L. Montano, "Blood, urine and semen volatile organic compound (voc) pattern analysis for assessing health environmental impact in highly polluted areas in italy," Environ. Pollut. **286**, 117410 (2021).
4. Z. He, X. Wang, Z. Ling, J. Zhao, H. Guo, M. Shao, and Z. Wang, "Contributions of different anthropogenic volatile organic compound sources to ozone formation at a receptor site in the pearl river delta region and its policy implications," Atmos. Chem. Phys. **19**(13), 8801–8816 (2019).
5. T. Salthammer, "Very volatile organic compounds: an understudied class of indoor air pollutants," Indoor Air **26**(1), 25–38 (2016).
6. L. Manti and A. D'Arco, "Cooperative biological effects between ionizing radiation and other physical and chemical agents," Mutat. Res. Mutat. Res. **704**(1-3), 115–122 (2010).
7. A. Al-Dabbous, A. K. S. Al-Tamimi, M. Shalash, A. Bajoga, and M. Malek, "Oxides of carbon, particulate matters and volatile organic compounds impact on indoor air quality during waterpipe smoking," Int. J. Environ. Sci. Technol. **16**(6), 2849–2854 (2019).
8. M. A. Bari and W. B. Kindzierski, "Concentrations, sources and human health risk of inhalation exposure to air toxics in edmonton, canada," Chemosphere **173**, 160–171 (2017).
9. M. A. Bari and W. B. Kindzierski, "Ambient volatile organic compounds (vocs) in communities of the athabasca oil sands region: Sources and screening health risk assessment," Environ. Pollut. **235**, 602–614 (2018).
10. V. Galstyan, A. D'Arco, M. D. Fabrizio, N. Poli, S. Lupi, and E. Comini, "Detection of volatile organic compounds: From chemical gas sensors to terahertz spectroscopy," Rev. Anal. Chem. **40**(1), 33–57 (2021).
11. V. Galstyan, "Quantum dots: Perspective in next-generation chemical sensors – a review," Anal. Chim. Acta **1152**, 238192 (2021).
12. W.-T. Koo, J.-S. Jang, and I.-D. Kim, "Metal-organic frameworks for chemiresistive sensors," Chem **5**(8), 1938–1963 (2019).
13. M. Krommweh, A. J. Schmithausen, H. F. Deeken, W. Büscher, and G.-C. Maack, "A new experimental setup for measuring greenhouse gas and volatile organic compound emissions of silage during the aerobic storage period in a special silage respiration chamber," Environ. Pollut. **267**, 115513 (2020).
14. P. Spanel and D. Smith, "Selected ion flow tube: A technique for quantitative trace gas analysis of air and breath," Med. Biol. Eng. Comput. **34**(6), 409–419 (1996).
15. M. Phillips, J. Herrera, S. Krishnan, M. Zain, J. Greenberg, and R. N. Cataneo, "J. Chromatogr., Biomed. Appl.," Journal of Chromatography B: Biomedical Sciences and Applications **729**(1-2), 75–88 (1999).
16. A. Fosnight, B. L. Moran, and I. R. Medvedev, "Chemical analysis of exhaled human breath using a terahertz spectroscopic approach," Appl. Phys. Lett. **103**(13), 133703 (2013).
17. S. Kanan, O. M. El-Kadri, I. Abu-Yousef, and M. C. Kanan, "Semiconducting metal oxide based sensors for selective gas pollutant detection," Sensor **9**(10), 8158–8196 (2009).

Optics EXPRESS

18. V. Galstyan, A. Ponzoni, I. Kholmanov, M. N. Natile, E. Comini, S. Nematov, and G. Sberveglieri, "Investigation of reduced graphene oxide and a nb-doped tio2 nanotube hybrid structure to improve the gas-sensing response and selectivity," ACS Sens. **4**(8), 2094–2100 (2019).
19. V. Galstyan, N. Poli, A. D'Arco, S. Macis, S. Lupi, and E. Comini, "A novel approach for green synthesis of wo3 nanomaterials and their highly selective chemical sensing properties," J. Mater. Chem. A **8**(39), 20373–20385 (2020).
20. R. Chu, C. Guan, Y. Bpo, J. Shi, Z. Zhu, P. Li, J. Yang, and L. Yuan, "All-optical graphene-oxide humidity sensor based on a side-polished symmetrical twin-core fiber michelson interferometer," Sens. Actuators, B **284**, 623–627 (2019).
21. Y. K. Mougang, L. D. Zazzo, M. Minieri, R. Capuano, A. Catini, J. M. Legramante, R. Paolesse, S. Bernardini, and C. D. Natale, "Sensor array and gas chromatographic detection of the blood serum volatolomic signature of covid-19," iScience **24**(8), 102851 (2021).
22. L. Wang, K. Kalyanasundaram, M. Stanacevic, and P. Gouma, "Nanosensor device for breath acetone detection," Sens. Lett. **8**(5), 709–712 (2010).
23. S. Chang, T.-J. Hsueh, I.-C. Chen, S.-F. Hsieh, S.-P. Chang, C.-L. Hsu, Y.-R. Lin, and B.-R. Huang, "Highly sensitive zno nanowire acetone vapor sensor with au adsorption," IEEE Trans. Nanotechnol. **7**(6), 754–759 (2008).
24. F. Radica, G. D. Ventura, L. Malfatti, M. C. Guidi, A. D'Arco, A. Grilli, A. Marcelli, and P. Innocenzi, "Real-time quantitative detection of styrene in atmosphere in presence of other volatile-organic compounds using a portable device," Talanta **233**, 122510 (2021).
25. S. Mou, A. D'Arco, L. Tomarchio, M. D. Fabrizio, A. Curcio, S. Lupi, and M. Petrarca, "Simultaneous elliptically and radially polarized thz from one-color laser-induced plasma filament," New J. Phys. **23**(6), 063048 (2021).
26. A. Balerna, S. Bartocci, G. Batignani, A. Cianchi, E. Chiadroni, and M. Coreno, "The potential of eupraxiasparc_lab for radiation based techniques," Condens. Matter **4**(1), 30 (2019).
27. A. Curcio, V. Dolci, S. Lupi, and M. Petrarca, "Terahertz-based retrieval of the spectral phase and amplitude of ultrashort laser pulses," Opt. Lett. **43**(4), 783–786 (2018).
28. A. Curcio, A. Marocchino, V. Dolci, S. Lupi, and M. Petrarca, "Resonant plasma excitation by single-cycle thz pulses," Sci. Rep. **8**(1), 1052 (2018).
29. A. Curcio, S. Mou, L. Palumbo, S. Lupi, and M. Petrarca, "Selection rules for the orbital angular momentum of optically produced thz radiation," Opt. Lett. **46**(7), 1514–1517 (2021).
30. A. D'Arco, M. D. Fabrizio, V. Dolci, A. Marcelli, M. Petrarca, G. D. Ventura, and S. Lupi, "Characterization of volatile organic compounds (vocs) in their liquid-phase by terahertz time-domain spectroscopy," Biomed. Opt. Express **11**(1), 1–7 (2020).
31. A. D'Arco, M. D. Fabrizio, V. Dolci, M. Petrarca, and S. Lupi, "Thz pulsed imaging in biomedical applications," Condens. Matter **5**(2), 25 (2020).
32. M. D. Fabrizio, A. D'Arco, S. Mou, L. Palumbo, M. Petrarca, and S. Lupi, "Performance evaluation of a thz pulsed imaging system: Point spread function, broadband thz beam visualization and image reconstruction," Appl. Sci. **11**(2), 562 (2021).
33. A. D'Arco, L. Tomarchio, V. Dolci, P. D. Pietro, A. Perucchi, S. Mou, M. Petrarca, and S. Lupi, "Broadband anisotropic optical properties of the terahertz generator hmq-tms organic crystal," Condens. Matter **5**(3), 47 (2020).
34. T. Mancini, R. Mosetti, A. Marcelli, M. Petrarca, S. Lupi, and A. D'Arco, "Terahertz spectroscopic analysis in protein dynamics: Current status," Radiation **2**(1), 100–123 (2022).
35. M. Naftaly, N. Vieweg, and A. Deninger, "Industrial applications of terahertz sensing: State of play," Sensors **19**(19), 4203 (2019).
36. K. Su, L. Moeller, R. Barat, and J. Federici, "Experimental comparison of terahertz and infrared data signal attenuation in dust clouds," J. Opt. Soc. Am. A **29**(11), 2360–2366 (2012).
37. Y. Hsieh, S. Nakamura, D. Abdelsalam, T. Minamikawa, Y. Mizutani, H. Yamamoto, T. Iwata, F. Hindle, and T. Yasui, "Dynamic terahertz spectroscopy of gas molecules mixed with unwanted aerosol under atmospheric pressure using fiber-based asynchronous-optical-sampling terahertz time-domain spectroscopy," Sci. Rep. **6**(1), 28114 (2016).
38. N. Shimizu, T. Ikari, K. Kikuchi, K. Matsuyama, A. Wakatsuki, S. Kohjiro, and R. Fukasawa, "Remote gas sensing in full-scale fire with sub-terahertz waves," 2011 IEEE MTT-S International Microwave Symposium p. 12180790 (2011).
39. J. Choi, S. Ryu, W. Kwon, K.-S. Kim, and S. Kim, "Compound explosives detection and component analysis via terahertz time-domain spectroscopy," J. Opt. Soc. Korea **17**(5), 454–460 (2013).
40. R. Smith and M. Arnold, "Selectivity of terahertz gas-phase spectroscopy," Anal. Chem. **87**(21), 10679–10683 (2015).
41. I. Medvedev, R. Schueler, J. Thomas, O. Kenneth, H. Nam, N. Sharma, Q. Zhoug, D. Lary, and P. Raskin, "Analysis of exhaled human breath via terahertz molecular spectroscopy.," *41st International Conference on Infrared, Millimeter, and Terahertz waves (IRMMW-THz)* p. 16502707 (2016).
42. N. Rothbart, O. Holz, R. Koczulla, K. Schmalz, and H. Hübers, "Analysis of human breath by millimeter-wave/terahertz spectroscopy," Sensors **19**(12), 2719 (2019).
43. K. Schmalz, N. Rothbart, P. Neumaier, J. Borngraber, H. Hübers, and D. Kissinger, "Gas spectroscopy system for breath analysis at mm-wave/thz using sige bicmos circuits," IEEE Trans. Microwave Theory Tech. **65**(5), 1807–1818 (2017).

Optics EXPRESS

44. J. Federici, B. Schulkin, F. Huang, D. Gary, R. Barat, F. Oliveira, and D. Zimdars, "Thz imaging and sensing for security applications-explosives, weapons and drugs," Semicond. Sci. Technol. **20**(7), S266–S280 (2005).
45. D.-Y. Kong, X.-J. Wu, B. Wang, Y. Gao, J. Dai, L. Wang, C.-J. Ruan, and J.-G. Miao, "High resolution continuous wave terahertz spectroscopy on solid-state samples with coherent detection," Opt. Express **26**(14), 17964–17976 (2018).
46. A. Deninger, A. Roggenbuck, S. Schindler, and S. Preu, "2.75 thz tuning with a triple-dfb laser system at 1550 nm and ingaas photomixers," J. Infrared, Millimeter, Terahertz Waves **36**(3), 269–277 (2015).
47. J. Demers, F. Garet, and J. Coutaz, "Atmospheric water vapor absorption recorded ten meters above the ground with a drone mounted frequency domain thz spectrometer," IEEE Sens. Lett. **1**(3), 1–3 (2017).
48. J. Demers, F. Garet, and J. Coutaz, "A uav-mounted thz spectrometer for real-time gas analysis," Proc. SPIE **10531**, 105310K (2018).
49. N. Rothbart, K. Schmalz, and H. Hübers, "A portable terahertz/millimeter-wave spectrometer based on sige bicmos technology for gas sensing applications," *In 2020 45th International Conference on Infrared, Millimeter, and Terahertz Waves (IRMMW-THz)* pp. 1–2 (2020).
50. T. Rice, M. A. Z. Chowdhury, M. W. Mansha, M. M. Hella, I. Wilke, and M. A. Oehlschlaeger, "Voc gas sensing via microelectronics-based absorption spectroscopy at 220-330 ghz," Appl. Phys. B **126**(9), 152 (2020).
51. A. Tekawade, T. E. Rice, M. A. Oehlschlaeger, M. W. Mansha, K. Wu, M. M. Hella, and I. Wilk, "Towards realization of quantitative atmospheric and industrial gas sensing using thz wave electronics," Appl. Phys. B **124**(6), 105 (2018).
52. R. Safian, G. Ghazi, and N. Mohammadian, "Review of photomixing continuous-wave terahertz systems and current application trends in terahertz domain," Opt. Eng. **58**(11), 1 (2019).
53. D. M. Slocum, L. H. Xu, R. H. Giles, and T. M. Goyette, "Retrieval of methanol absorption parameters at terahertz frequencies using multispectral fitting," J. Mol. Spectrosc. **318**, 12–25 (2015).
54. H. S. Müller, F. Schlöder, J. Stutzki, and G. Winnewisser, "The cologne database for molecular spectroscopy, cdms: a useful tool for astronomers and spectroscopists," J. Mol. Struct. **742**(1-3), 215–227 (2005).
55. R. Kakar and C. Quade, "Microwave rotational spectrum, and internal rotation in gauche ethyl alcohol," J. Chem. Phys. **72**(8), 4300–4307 (1980).
56. S. Kondo and E. Hirota, "Microwave spectrum and internal rotation of isopropyl alcohol," J. Mol. Spectrosc. **34**(1), 97–107 (1970).
57. C. Russo, A. D'Anna, A. Ciajolo, and M. Sirignano, "The effect of butanol isomers on the formation of carbon particulate matter in fuel-rich premixed ethylene flames," Combust. Flame **199**, 122–130 (2019).
58. F. Piccirilli, F. Tardani, A. D'Arco, G. Birarda, L. Vaccari, S. Sennato, S. Casciardi, and S. Lupi, "Infrared nanospectroscopy reveals dna structural modifications upon immobilization onto clay nanotubes," Nanomaterials **11**(5), 1103 (2021).
59. H. Yang, S. Yang, J. Kong, A. Dong, and S. Yu, "Obtaining information about protein secondary structures in aqueous solution using fourier transform ir spectroscopy," Nat. Protoc. **10**(3), 382–396 (2015).
60. F. G. G. D. Ventura and A. Marcelli, "Mobile monitoring of particulate matter: State of art and perspectives," Atmos. Pollut. Res. **7**(2), 228–234 (2016).
61. A. Hassani and M. Skorobogatiy, "Surface plasmon resonance-like integrated sensor at terahertz frequencies for gaseous analytes," Opt. Express **16**(25), 20206–20214 (2008).
62. G. Mishra, D. Kumar, V. Chaudhary, and S. Sharma, "Terahertz refractive index sensor with high sensitivity based on two-core photonic crystal fiber," Microw. Opt. Technol. Lett. **63**(1), 24–31 (2021).
63. D. Vogt, A. Jones, and R. Leonhardt, "Terahertz gas-phase spectroscopy using a sub-wavelength thick ultrahigh-q microresonator," Sensors **20**(10), 3005 (2020).
64. S. Acharyya, B. Jana, S. Nag, G. Saha, and P. Guha, "Single resistive sensor for selective detection of multiple vocs employing sno2 hollowspheres and machine learning algorithm: A proof of concept," Sens. Actuators, B **321**, 128484 (2020).